Reflectivity around the gold L-edges of X-ray reector of the soft X-ray telescope onboard ASTRO-H

Maeda, Yoshitomo; Kikuchi, Naomichi; Kurashima, Sho; Ishida, Manabu; Iizuka, Ryo; Hayashi, Takayuki; Okajima, Takashi; Matsumoto, Hironori; Mitsuishi, Ikuyuki; Saji, Shigetaka

Total number of authors:
17

Published in:
Optics for EUV, X-Ray, and Gamma-Ray Astronomy VIII

Link to article, DOI:
10.1117/12.2275605

Publication date:
2017

Document Version
Publisher's PDF, also known as Version of record

PROCEEDINGS OF SPIE

SPIEDigitalLibrary.org/conference-proceedings-of-spie

The Hitomi (ASTRO-H) Soft X-ray Telescope (SXT): current status of calibration

Yoshitomo Maeda, Naomichi Kikuchi, Sho Kurashima, Manabu Ishida, Ryo Iizuka, et al.

Yoshitomo Maeda, Naomichi Kikuchi, Sho Kurashima, Manabu Ishida, Ryo Iizuka, Takayuki Hayashi, Takashi Okajima, Hironori Matsumoto, Ikuyuki Mitsuishi, Shigetaka Saji, Toshiki Sato, Sasagu Tachibana, Hideyuki Mori, Finn Christensen, Nicolai Brejnholt, Kiyofumi Nitta, Tomoya Uruga, "The Hitomi (ASTRO-H) Soft X-ray Telescope (SXT): current status of calibration," Proc. SPIE 10399, Optics for EUV, X-Ray, and Gamma-Ray Astronomy VIII, 103990Q (29 August 2017); doi: 10.1117/12.2275605

SPIE.

Event: SPIE Optical Engineering + Applications, 2017, San Diego, California, United States

Reflectivity around the gold L-edges of x-ray reflector of the soft x-ray telescope onboard ASTRO-H

Yoshitomo Maeda[a,b], Naomichi Kikuchi[b,c], Sho Kurashima[b,c], Manabu Ishida[a,b,c], Ryo Iizuka[a], Takayuki Hayashi[d,e], Takashi Okajima[d], Hironori Matsumoto[e], Ikuyuki Mitsuishi[e], Shigetaka Saji[e], Toshiki Sato[b,c], Sasagu Tachibana[e], Hideyuki Mori[d], Finn Christensen[f], Nicolai Brejnholt[g], Kiyofumi Nitta[h], and Tomoya Uruga[h]

[a]Institute of Space and Astronautical Science (ISAS),Japan Aerospace Exploration Agency (JAXA), 3-1-1 Yoshinodai, Sagamihara, 229-8510, Japan
[b]The Graduate University for Advanced Studies, 3-1-1 Yoshinodai, Sagamihara, 229-8510, Japan
[c]Tokyo Metropolitan University, 1-1 Minami-Osawa, Hachioji, Tokyo 192-0397 , Japan
[d]NASA Goddard Space Flight Center, Code 662, Greenbelt, MD 20771, U.S.A
[e]Nagoya University, Furo-cho, Chikusa-ku, Nagoya 464-8602, Japan
[f]DTU Space, National Space Institute, Technical University of Denmark, Elektrovej 327, DK-2800 Lyngby, Denmark
[g]Lawrence Livermore National Laboratory, Livermore, CA 94550, U.S.A.
[h]JASRI/SPring-8, Sayo-cho, Sayo, Hyogo 679-5198, Japan

ABSTRACT

We report the atomic scattering factor in the 11.2–15.4 keV for the ASTRO-H Soft X-ray Telescope (SXT)[9] obtained in the ground based measurements. The large effective area of the SXT covers above 10 keV. In fact, the flight data show the spectra of the celestical objects in the hard X-ray band. In order to model the area, the reflectivity measurements in the 11.2–15.4 keV band with the energy pitch of 0.4 – 0.7 eV were made in the synchrotron beamline Spring-8 BL01B1. We obtained atomic scattering factors f1 and f2 by the curve fitting to the reflectivities of our witness sample. The edges associated with the gold′s L-I, II, and III transitions are identified, of which the depths are found to be roughly 60% shallower than those expected from the Henke's atomic scattering factor.

Keywords: X-rays, ASTRO-H/*Hitomi*, Soft X-ray Telescopes (SXTs), Wolter Type-I optics, stray lights

1. INTRODUCTION

The international X-ray observatory ASTRO-H,[13] later renamed HITOMI, was launched on February 17, 2016(JST). Two Soft X-ray Telescopes (SXT-I and SXT-S) are mounted on the ASTRO-H satellite,[12] see also Okajima et al. in this volume[9] for its flight performance. The SXT-I and SXT-S focus X-ray images on the respective focal plane detectors of the CCD camera (SXI) and the micro-calorimeter (SXS).

The SXTs adopt the Wolter-I type optics with the reflector surface coated with gold. One of the hurdles in constructing the SXT response is to obtain the accurate reflectivity around the complex gold L edges, which appear in the 11–15 keV band. One of the issues of the SXTs response construction is then to know the reflectivity around the gold L edges that appears in the 11-15 keV band. In order to model the effective-area curve in the edge bands, the reflectivity of the SXT's gold surface with a precise energy pitch should be measured, on which we focus in this paper. Other issues are, and will be, separately addressed in our companion papers, such as Iizuka R. et al.,[3] Sato T. et al.,[10] Sato T. et al. in this volume,[11] Kurashima S. et al. in this volume,[7] Hayashi, T. et al. in this volume,[1] and Okajima, T. et al. in this volume.[9]

Yoshitomo Maeda: E-mail: iizuka@astro.isas.jaxa.jp, ymaeda@astro.isas.jaxa.jp

Optics for EUV, X-Ray, and Gamma-Ray Astronomy VIII, edited by Stephen L. O'Dell, Giovanni Pareschi, Proc. of SPIE Vol. 10399, 103990Q · © 2017 SPIE · CCC code: 0277-786X/17/$18 · doi: 10.1117/12.2275605

The energy resolution of the focal plane detector SXS-XCS of the ASTRO-H SXT-S is as good as ∼5 eV at 6 keV, which corresponds to the resolution power of ∼ 1000.[4] The reflectivity with an energy pitch with a few eV or better is required for the calculation of the effective area of the SXT.

Motivated with this, we have conducted the pre-flight experiment to measure the reflectivity of the reflectors of the ASTRO-H SXT for the energy range of 11–15 keV, using a synchrotron beamline at Spring-8. We here present the result of our experiment, in which we have accomplished the finest energy-pitch measurements of 0.4–0.7 eV, ever reported at this energy range for the SXT reflector. The results given here was submitted to the Optical Express journal as Kikuchi et al.[5]

2. EXPERIMENT

Details of our experiment will be reported in Kikuchi et al. (2016).[5] We then picked up the principles of the measurements for the reflectivity and the atomic scattering factor from the literature.

2.1 Reflectivity of a mono layer

The X-ray reflectivity of a mono layer is known to be dependent on the physical condition of the incident X-rays and the layers. The reflectivity is given by the following equation, using the Nevot-Croce exponential factor,[8] which takes into account the effect of the surface roughness on X-ray scattering,

$$R = R_0 \exp\left(-n_i n_j \sin\theta_i \sin\theta_j \left(\frac{4\pi\sigma}{\lambda}\right)^2\right) \tag{1}$$

where R_0 is the ideal surface reflectivity calculated with the Fresnel equations, n_i and n_j are indices of refraction between the two layers, θ_i and θ_j are the incident and reflected angles of X-rays, and σ is the surface roughness. If the vacuum atmosphere for the incident space and specular reflection ($\theta_i = \theta_j = \theta$) are assumed, the equation 1 is simplified as

$$R = R_0 \exp\left(-n \sin^2\theta \left(\frac{4\pi\sigma}{\lambda}\right)^2\right). \tag{2}$$

The complex refractive index of a layer consisting of a single element is

$$\tilde{n} = 1 - \delta - i\beta \tag{3}$$

$$\tag{4}$$

where δ and β are related to the atomic scattering factors f1 and f2 via equations

$$\delta = \frac{N_a r_e}{2\pi}\lambda^2 f_1 \tag{5}$$

$$\beta = \frac{N_a r_e}{2\pi}\lambda^2 f_2 \tag{6}$$

and

$$N_a = (N_0/A)\rho \tag{7}$$

with the Avogadro constant N_0, a classical electron radius r_e, an atomic number A, a mass density ρ, and an X-ray wavelength λ.

The ideal surface reflectivity R_0 is then calculated as

$$R_0 = \frac{h - \frac{\theta}{\theta_c}\sqrt{2(h-1)}}{h + \frac{\theta}{\theta_c}\sqrt{2(h-1)}} \tag{8}$$

$$h = \left(\frac{\theta}{\theta_c}\right)^2 + \sqrt{\left(\left(\frac{\theta}{\theta_c}\right)^2 - 1\right)^2 + \left(\frac{\beta}{\delta}\right)^2} \tag{9}$$

where θ_c is a critical angle and is given by

$$\theta_c = \sqrt{2\delta}. \tag{10}$$

(11)

In summary, the reflectivity is a function of the energy (E or wavelength λ), incident angle (θ) of X-rays and roughness (σ), and density (ρ) and the atomic scattering factors ($f1$ and $f2$) of the surface layer. In order to obtain all these parameters for the ASTRO-H SXT reflector, we measure the reflectivity, using the witness sample.

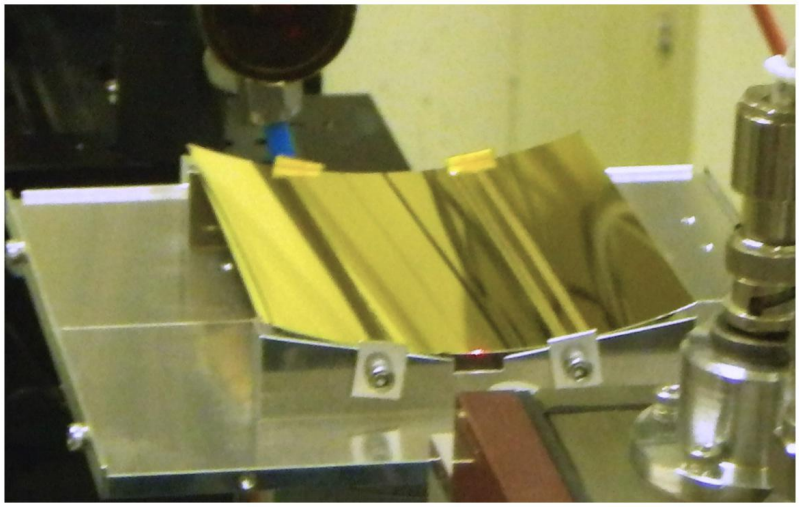

Figure 1. Photo of our witness sample.[5] Details are summarized in Table 1.

Table 1. Sample Reflector

Type		Replica Foil
Layers		Gold ∼2000[Å] / Epoxy 10μm / Aluminum 152 μm
Size	Height	101.6 [mm]
	Width	88 [mm]
	Radius	114 [mm]

2.2 Measurements

2.2.1 Spring-8 BL01B1

X-ray reflectivity was measured at the BL01-B1 beam line at the SPring-8 facility of the Japan Synchrotron Radiation Research Institute (Proposal numbers 2014A1471/2014B1475).

The incident beam from the ring is reflected at two gracing angle mirrors and two crystals. From the ring side, the first collimating mirror, the first crystal, the second crystal and the second focusing mirror are positioned in this order. The two mirrors are positioned in front and rear of the two crystals.

For the material for the diffraction plane, Si(111) double-crystals (d = 1.63747Å) were chosen to cover the energy range of 9–16 keV. A typical photon flux at the position of a sample for a beam size of 10 mm (horizontal)

$\times$ 0.2 mm (vertical) is 1×10^9–2×10^{10} photon s^{-1} in 7.1–72 keV. The energy resolution of the beam is $\Delta E/E \sim 3\times10^{-5}$ (FWHM), which corresponds to 0.3 eV at $\sim$ 10 keV.

The second mirror is designed to focus the beam to $\sim$0.3 mm in height at the sample, which is located at 4.9 m away from the sample reflector. The mirrors are tilted to cut out high-energy photons; the tilt angle is tuned within the critical angle for the energy of $\sim$20 keV (=3mrad). In the energy band of 9–16 keV, the higher harmonics are negligible. The diverging angle of the incident beam is limited with the viewing angle of the 1 m long second mirror viewed from the sample, which is about 0.04 degrees in full width.

The ion chambers are used to detect X-rays. One chamber (I0) is mounted between the beam slit and the sample, whereas the other (I1) is mounted at the end. The output current of the ion chambers are read out with a current amplifier Keithley Current Amplifier 428. The output voltage is sent to the low-pass filter electronics and then is converted to a digital number with a combination of a voltage-frequency converter and a counter. Finally, we read the output counts of the ion chambers I0 and I1, and determine transmissivity of the foils and reflectivity of the reflectors.

2.2.2 Energy calibration

The calibration of the relation between the crystal angle and the energy was based on identification of the pre-edge of the Cu-K absorption at $\sim$8.979 keV with the 1s$-$ $>$3d(+4p) transition. The 6μm-thick Cu film is used for the calibrator. We identified the local minimum of the derivatives as the Cu-K pre-edge. We then gave an offset of the crystal rotation stage to match the energy at the minimum as 8980.48 eV.[6] A typical error of the energy at the minimum is $\sim$1 eV,. We interpret this error as the systematic uncertainty of the incident energy in our experiment in 11.2–15.4 keV. The offset is applied throughout our measurements.

2.2.3 Sample Stages and Detectors

Our sample "reflector" (Figure 1) is put on near the focus of the 2nd focusing mirror. In front and rear of the reflector, two ion chambers, designated respectively as I0 and I1, are placed. Four-jaw slits are installed in front of each ion chamber. A He pass tube with $\sim$ 40mm long is installed between I0 and the reflector in order to reduce the attenuation by air.

The reflector is put on a rotation θ-stage, whereas the four-jaw slit in front of I1 is on the 2θ-stage. The incident beam is shaped to 0.05 mm $\times$ 1 mm for the vertical (V) and horizontal (H) directions, respectively. The reflected beam passes through the 2nd four-jaw slit with 6 (V) mm $\times$ 1 (H) mm in front of the I1 detector. The position of the I1 detector is fixed. Regardless of the variable position of the slit on the 2θ-stage, it can accumulate the photons since the window vertical width is $\sim$63 mm wide.

With the computer-controlled stages and detectors, the reflectivity is measured with the following four steps,

1. Measure the flux of the reflected beam ($I_{\rm Ref}(E,\theta)$), which includes the detector background and scattering at the air.
2. Remove sample and measure the flux of the direct beam ($I_{\rm Drt}(E,\theta)$), which includes the detector background and scattering at the air. The scattering should be negligible.
3. (Remove sample and) measure the flux of the reflected beam. X-rays do not illuminate the reflector. The scatting at the air in the beam path is measured ($I_{\rm Scat}(E,\theta)$). The detector background is included.
4. Stop the beam and measure the detector background ($I_{\rm Bkg}(E,\theta)$).

The reflectivity R is then calculated as

$$R = (\frac{I1_{\rm Ref} - I1_{\rm Scat}}{I0_{\rm Ref} - I0_{\rm Scat}})/(\frac{I1_{\rm Drt} - I1_{\rm Bkg}}{I0_{\rm Drt} - I0_{\rm Bkg}}). \quad (12)$$

Two methods are conceivable for obtaining the reflectivity at a given energy E and at a given angle θ: angle scanning with the fixed energy (the angular scan) and energy scanning with the fixed angle (the energy scan).

The angular scan is sensitive to all the surface parameters; thus we first performed an angular scan to determine the roughness and the density, as well as the atomic scattering factors. However, due to the limited machine time of the beamline, we could not measure the angular reflectivity with a fine energy-interval for the wide energy band of 11.2–15.2 keV. We then made an energy scan at ten incident angles and obtained the angular reflectivity at each angle.

3. ANALYSIS AND RESULTS

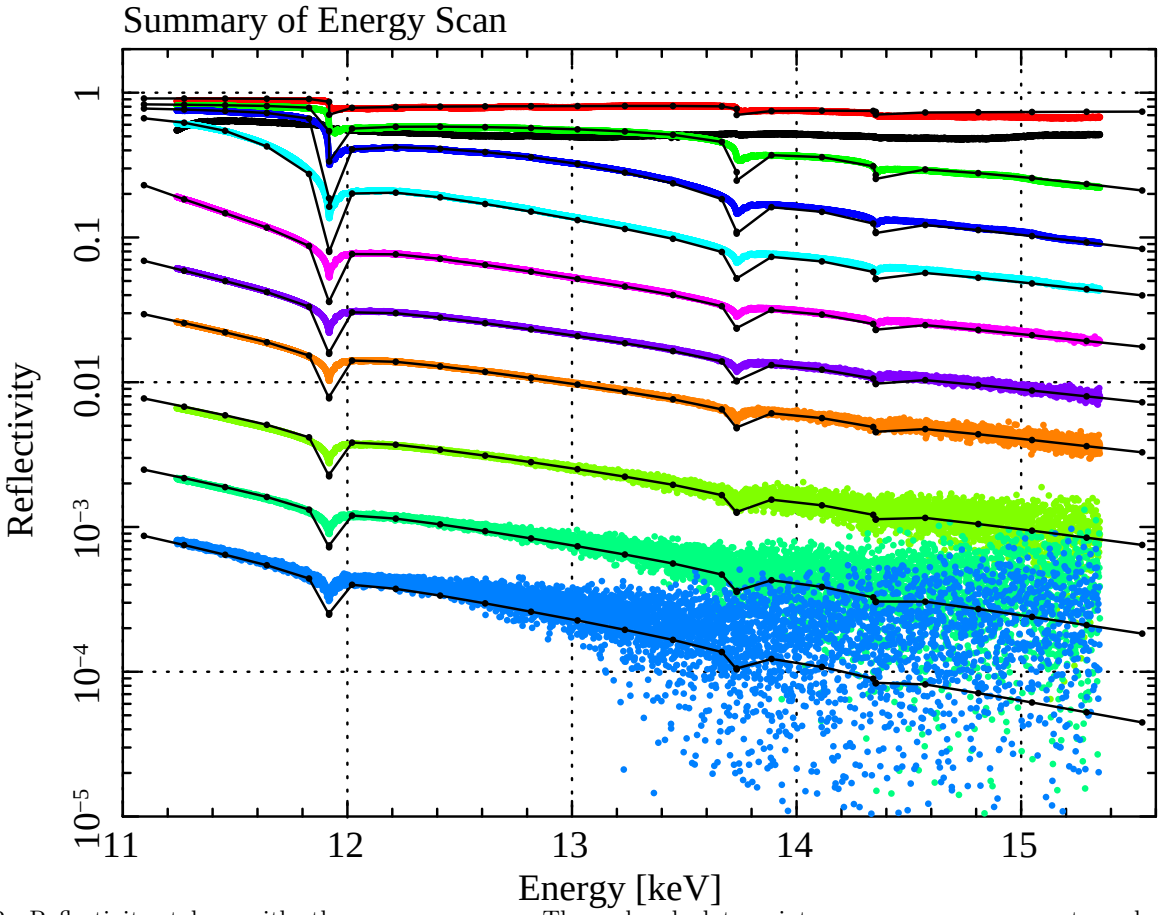

Figure 2. Reflectivity taken with the energy scan. The colored data-points are our measurements, whereas the black data-points are calculated, using the HENKE table. From top to bottom, the incident angles are 0.20,0.30,0.33,0.36,0.40,0.45,0.50,0.60,0.70 and 0.80 degrees, respectively. The errors are in 1-σ confidence.

The reflectivity is obtained with the equation 12. Figure 2 plots the reflectivity obtained with the energy-scan. We obtained energy-pitch measurements of 0.4–0.7 eV for the SXT reflector, the finest ever reported in the 11.2 – 15.2 keV range were obtained. The edges associated with the L-I, II, and III transitions are identified (Figure 3), of which the depths are found to be roughly 60% shallower than those expected from Henke's atomic scattering factors[2] .

Since the number of the angular data-points is limited, we fixed the roughness and density to be those obtained with the angular scan data and fit them with the two free parameters f1 and f2. The best-fit atomic scattering factors are shown in Figure 4 and in the supplemetary table.

Our measurement is in good agreement with the HENKE table[2] in the energy band between 12.2 and 13.4 keV. However, it shows a prominent discrepancy at the edge energies (L_I at 14.3528 keV, L_{II} at 13.7336 keV,

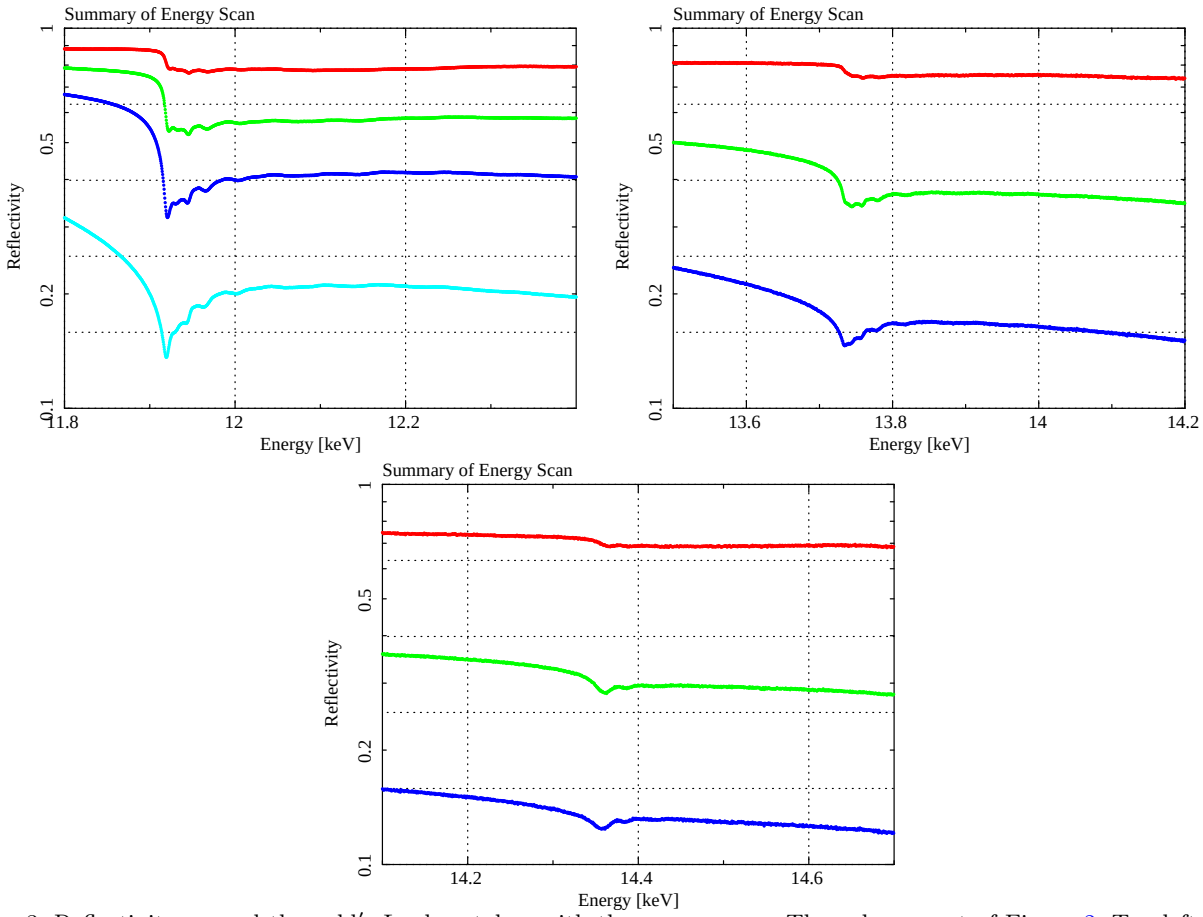

Figure 3. Reflectivity around the gold′s L-edges taken with the energy scan. The enlargement of Figure 2 .Top left: L3 edge. Top right: L2 edge. Bottom: L1 edge. From top to bottom, the incident angles are 0.20 (red) ,0.30 (green), 0.33(blue) , and 0.36 (cyan) degrees, respectively.

L_{III} at 11.9187 keV), which is probably due to the energy pitch in our measurements being finer than that in the Henke table. In the f2 factor, the fine structure around the gold L_{III} edge is visible at 12 keV (Figure 3). It is identified as the XAFS structures of gold. Similar discrepancies can be spotted at the deepest structures in the other edges of L_{II} and L_I, but are marginal due to the systematics. Our measured f2 factors are found to be overall consistent with those in the Henke table within the margin of error except near the XAFS structures at L_{III} edges. We should note that the f2 factor at the energy above 14 keV is poorly constrained due to systematics.

4. CONCLUSION

1. The reflectivity of the SXT's reflectors, which consist of a gold mono-layer, was measured for the energy range of 11.2–15.4 keV with the energy pitch of 0.4–0.7 eV.
2. The atomic scattering-factors f1 and f2 were determined with the unprecedented accuracy.
3. The uncertainty of this atomic scattering factors will be addressed using the flight data in future.

The authors are grateful to all the full-time engineers and part-time workers in the GSFC/NASA laboratory for support in mass production of the Soft X-ray Telescope reflectors. R.I. and Y.M. acknowledge support from the Grants-in-Aid for Scientific Research (numbers 25870744, 25105516 and 23540280) by the Ministry of Education, Culture, Sports, Science and Technology.

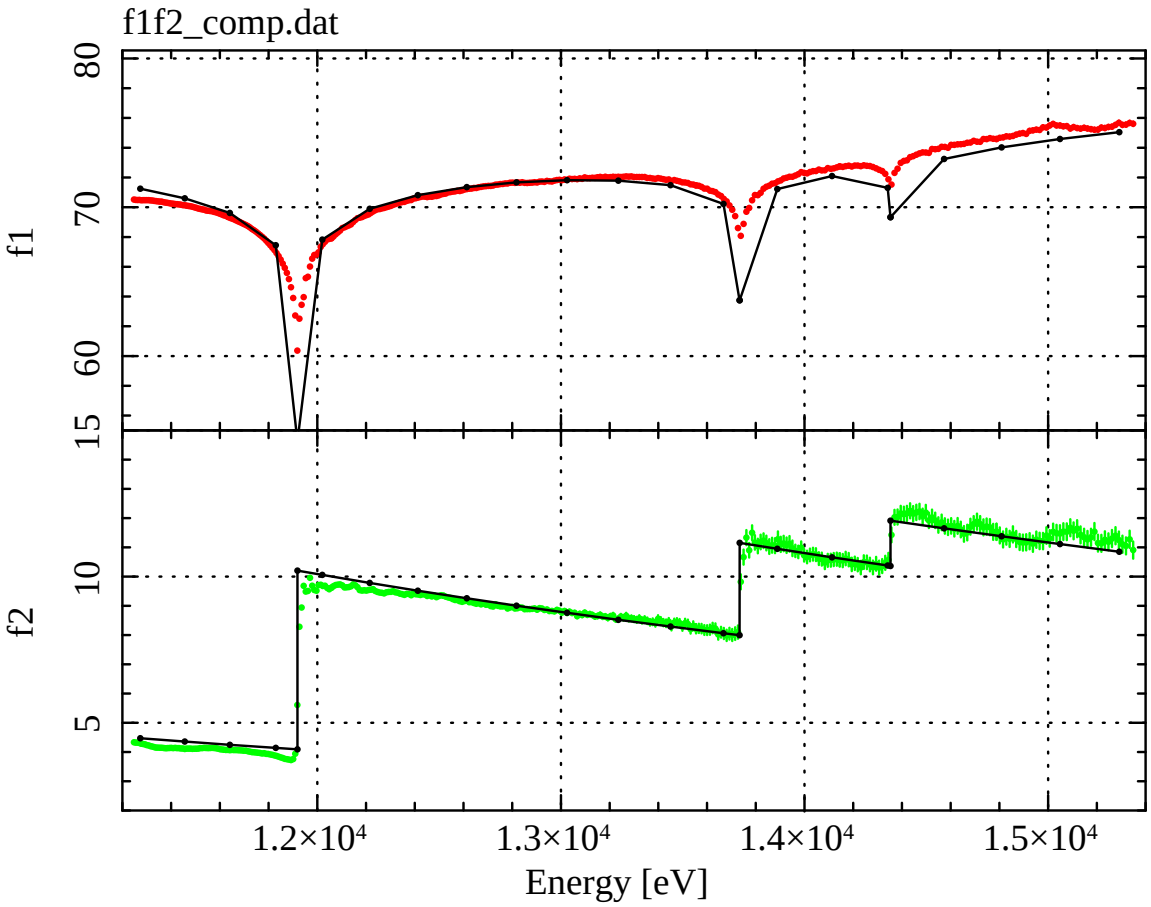

Figure 4. Preliminary atomic scattering factors f1 (upper panel) and f2 (lower panel). The red and green points show the factors obtained by the curve-fitting for the energy scans. The black points correspond to the numbers of the HENKE table. (See also Kikuchi et al. 2016)

REFERENCES

[1] T. Hayashi, et al. "Point spread function of ASTRO-H soft x-ray telescope (SXT)", Society of Photo-Optical Instrumentation Engineers (SPIE) Conference Series, this volume, submitted, (2016)

[2] B.L. Henke, E.M. Gullikson, and J.C. Davis. "X-ray interactions: photoabsorption, scattering, transmission, and reflection at E=50-30000 eV, Z=1- 92", Atomic Data and Nuclear Data Tables Vol. 54 (no.2), 181-342 (1993).

[3] R. Iizuka, T. Hayashi, Y. Maeda, M. Ishida, K. Tomikawa, T. Sato, N. Kikuchi, T. Okajima, Y. Soong, P. J. Serlemitsos, H. Mori, T. Izumiya, and S. Minami, "Ground-based x-ray calibration of the Astro-H soft xray telescopes", in Society of Photo-Optical Instrumentation Engineers (SPIE) Conference Series, vol. 9144 of Society of Photo-Optical Instrumentation Engineers (SPIE) Conference Series, vol. 9144 of Society of Photo-Optical Instrumentation Engineers (SPIE) Conference Series, p. 58. (2014)

[4] R. Kelley, et al. "The ASTRO-H high-resolution soft x-ray spectrometer", Society of Photo-Optical Instrumentation Engineers (SPIE) Conference Series, this volume, submitted, (2016)

[5] Kikuchi, N., et al., "Atomic scattering factor of the ASTRO-H (Hitomi) SXT reflector around the gold 's L edges", The Optical Express, submitted (2016)

[6] S. Kraft, J. Stümpel, P. Becker, and U. Kuetgens, "High resolution xray absorption spectroscopy with absolute energy calibration for the determination of absorption edge energies", Review of Scientific Instruments 67, 681 (1996)

[7] S. Kurashima, et al. "Reflectivity around the gold M-edges of x-ray reflector of the soft x-ray telescope onboard ASTRO-H", Society of Photo-Optical Instrumentation Engineers (SPIE) Conference Series, this volume, submitted, (2016)

[8] L. Nevot and P. Croce, "Caractérisation des surfaces par réflexion rasante de rayons X. Application à l'ètude du polissage de quelques verres silicates", Revue de Physique Appliquee, **15**(3), 761–779 (1980).

[9] T. Okajima, et al. "First peek of ASTRO-H soft x-ray telescope (SXT) in-orbit performance", Society of Photo-Optical Instrumentation Engineers (SPIE) Conference Series, this volume, submitted, (2016)

[10] T. Sato, et al. "Examining the angular resolution of the ASTRO-H Soft X-ray Telescopes", JATIS, submitted, (2016)

[11] T. Sato, et al. "The ASTRO-H SXT performance to the large off-set angles", Society of Photo-Optical Instrumentation Engineers (SPIE) Conference Series, this volume, submitted, (2016)

[12] Y. Soong, et al. "ASTRO-H Soft X-ray Telescope (SXT)", Society of Photo-Optical Instrumentation Engineers (SPIE) Conference Series 9144, 914428. (2014)

[13] T. Takahashi, et al., "The ASTRO-H X-ray astronomy satellite", Society of Photo-Optical Instrumentation Engineers (SPIE) Conference Series 9144, 914425. (2014)